CHARACTERISATION OF A LIQUID GAS INTERFACE DURING AN ATOMISATION PROCESS AT LOW WEBER NUMBER

Dr. K. Triballier, Dr. C. Dumouchel, Dr. J. Cousin

UMR 6614 – CNRS CORIA
Université et INSA de Rouen
76801 St Etienne du Rouvray Cedex, France
phone: (33) 2 32 95 36 23

ABSTRACT

The present work investigates the role of the internal flow on atomisation processes when the interaction between the liquid and the gas has no effect (low Weber number). According to the literature, the turbulent level at the nozzle exit mainly controls the atomisation efficiency in such conditions. A numerical and experimental study is conducted on a series of cavity nozzles, simplified geometry of compound nozzles based on the concept of atomisation controlled by turbulence. The work consisted in calculating the internal liquid flow and to measure the drop-size distribution for a wide range of working conditions. Furthermore, the atomising liquid flow is experimentally characterised by measuring the local liquid gas interface length. It is found that the turbulent level is not solely responsible for the atomisation efficiency and that the non-axial flow component plays a dominant role also. It is also shown that the role of the non-axial issuing flow component is not limited to influence the shape of the issuing liquid flow. The experimental characterisation of the local interface length appears relevant for atomisation process description. Indeed, this length makes appear a maximum that is found to be solely related to the Sauter mean diameter of the spray and to the part of the incident energy available for atomisation. This finding suggests that the approach that consists in describing liquid atomisation processes as a problem of liquid surface balance is relevant and very promising.

INTRODUCTION

In many situations of liquid atomisation in gaseous environment, the difference of velocity between the liquid and the gas is too small to expect any effect of the aerodynamic forces on the liquid flow disintegration and on the spray formation. For these situations, characterised by a low gaseous Weber number, the atomisation process depends mainly on the characteristics of the issuing liquid flow. Among the important flow characteristics, the turbulent level is known to promote atomisation and some low-pressure injectors are designed on this concept such as compound port fuel injectors for instance [1]. These injectors are usually constituted of a superposition of three disks whose aim is to impose complex flow passages to the liquid in order to increase the turbulent level and to promote atomisation. Many studies, either experimental or numerical, have been conducted on the performances of compound injectors [2-6]. They all agree to conclude that turbulent kinetic energy is the main factor that controls atomisation and that this energy depends mainly on the nozzle geometry. However, Glodowski et al. [4] concluded that the level of turbulent kinetic energy does not influence solely the droplet size and a more recent study [7] pointed out the dominant role of the non-axial liquid flow at the nozzle exit on the atomisation process.

The aim of the present study is to examine the role of the turbulence and of the non-axial flow component on the atomisation performances of low-Weber liquid flows. In order to promote the presence of these two flow characteristics, simplified cavity nozzles, directly inspired from the geometry of compound injectors, are experimentally and numerically investigated. Furthermore, all the studies quoted above investigated the performances of injectors by relating calculated issuing flow characteristics to a mean drop size of the spray measured at some distance from the nozzle, ignoring the liquid flow perturbation step. In the present analysis, it is intended to introduce a characterisation of the continuous perturbed liquid flow based on the following idea. An atomisation process can be seen as a process where the surface area between a given amount of liquid and the surrounding gas increases until a physical phenomenon opposes to this increase and imposes the break-up of the flow. When the aerodynamic effects are small, the liquid break-up is likely to be controlled by surface tension forces. Thus, the spatial evolution of the liquid gas interface as the flow goes downwards appears as a relevant characteristic of the atomisation process. The interface area is very difficult to measure since atomising liquid flows are 3D in nature. However, the local interface length can be determined in one direction thanks to the analysis of images of high spatial and temporal resolution. This quantity is believed to be representative of the amount of interface if the atomisation process is axisymmetric or if it is mainly 2D. The flows issuing from the simplified cavity nozzles studied in the present work show this latter characteristic.

EXPERIMENTAL AND NUMERICAL STUDIES

Experimental Study

The experimental part of this work investigates the behaviour of simplified cavity nozzles of different dimensions. These nozzles are composed of a superposition of three disks perforated by a circular hole (Fig. 1). The disk 1 through which the fluid enters the nozzle is kept constant. Three series of nozzles are available. They differ from their disk 2 thickness and eccentricity. The series 1 nozzles (S1) have a constant disk 2 thickness of 75 µm and the series 2 nozzles have a constant disk 2 thickness of 175 µm. For these two series, the eccentricity varies according to the values given in Table 1. The series 3 nozzles have a constant eccentricity of 200 µm and differ by the thickness of disk 2 according to the values given in table 1.

The experiments consist in visualising the liquid flow issuing from the nozzle and in measuring the drop-size distributions of the resulting sprays. The visualisation diagnostic was described in a previous paper [8]. It uses a combination of a digital camera with a high spatial resolution and a short duration light source to freeze the issuing liquid flow. The visualisations are used to measure the angle α_T of the liquid flow just at the nozzle exit and the local interface length L of the continuous flow. The angle is measured on 7.5 x 5 mm^2 images (1 pixel = 2.5 µm) and the local interface length is determined on 15 x 10 mm^2 images (1 pixel = 5 µm). The image analysing technique used to determine the angle and the interface length is applied on a minimum of 50 images for each configuration.

The local interface length measurement is conducted on instantaneous images that contain the continuous part of the liquid flow only. All the liquid elements (drops or ligaments) detached to the bulk flow are eliminated. The edge of the issuing liquid flow is delimited thanks to an edge-tracking algorithm. For each pixel of the contour, the distance to the previous edge pixel is measured. Basically, this distance can take two values only, namely 5 µm (1 pixel) or 7.07 µm ($\sqrt{2}$ pixel). The local interface length of the ith line (corresponding to the downstream position h = 5 x i µm) is defined as the sum of the distances between the contour pixel belonging to this line and their previous immediate neighbours. The interface length determined by this method is representative of the presence of interface perturbations. Indeed, straight interfaces would report a constant local length whose value is a function of the interface direction only. Although the projection of the liquid flow in one direction is considered only, this method is believed to report an information that is related to the local interface. The reason for this is that the images are taken in the direction perpendicular to the liquid flow expansion plane that is the same as the nozzle symmetric plane (plane of Fig. 1).

The drop-size distribution is measured with a Spraytec equipment. Based on the light diffraction technique, this diagnostic reports a volume-based drop-size distribution integrated in space and in time. The time integration aspect is not penalising in the present study as the injectors are used under steady state operation. Being interested by the primary spray drop-size distribution, the measurements are conducted as close as possible to the nozzle exit. Therefore, according to the injection pressure and to the nozzle configuration, the distance at which the drop-size distribution is measured varies from 14 mm to 26 mm. Finally, the Spraytec is equipped with a 450 mm focal length lens allowing the measurements of drop diameter ranging from 8.6 to 1 041 µm.

Throughout the experimental investigation the injection pressure is kept low and does not exceed 5 bar. All the experiments are performed with a single fluid whose physical properties are: density 760 kg/m^3, surface tension 24 mN/m, k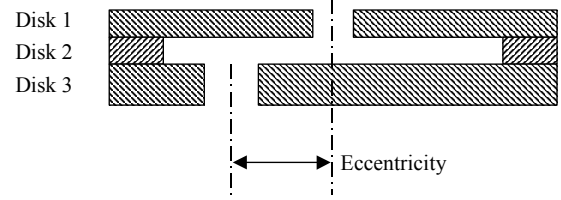inematic viscosity 1.312. 10^{-6} kg/ms. For each working condition, the mass flow rate is determined by weighting the amount of fluid collecting during a controlled time interval. These measurements are used to validate the internal flow simulations summarised in the following section.

Fig. 1. Design of the simplified cavity nozzle

	I1	I2	I3	I4	I5
Eccentiricities (for S1 and S2)	200	500	700	900	-
Disk 2 thickness (for S3)	75	125	153	175	200

Table 1. Dimensions of the nozzle disks (µm).

C_D	$= \dfrac{Q_v}{S\sqrt{\dfrac{2\Delta P_i}{\rho_L}}}$	(-)
E_k	$= \dfrac{\sum\limits_{j} vol_j \rho_L \left(u_j^2 + w_j^2\right)}{2\sum\limits_{j} vol_j}$	(kg/ms^2)
T_{ke}	$= \dfrac{\sum\limits_{j} vol_j \left(u_j'^2 + v_j'^2 + w_j'^2\right)}{2\sum\limits_{j} vol_j}$	(m^2/s^2)

Table 2. Definition of the issuing flow characteristics

Numerical Study

The numerical code Fluent 5.4 is used to calculate the flow that develops inside the nozzle. The methodology for the mesh creation and the models and boundary conditions used in the calculation were presented in a previous paper [8] and are not recalled here. It is just reminded that a RNG k-ɛ model is used to calculate the turbulence of the flow. Despite the fact that this model might not be appropriate since the turbulence is probably not fully developed, it is believed to give a good estimation of the energy contained in the turbulent component of the flow. Furthermore, studies of the literature dealing with the
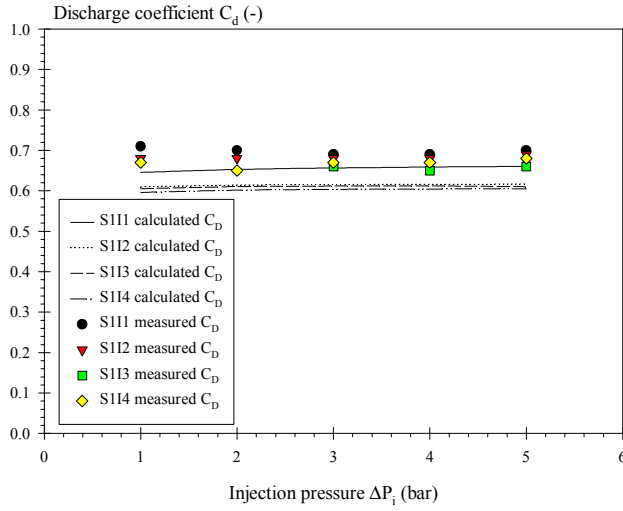
calculation of the flow that develops inside compound nozzles all used the turbulent k-ε model [4, 5, 7]. The issuing flow is characterised by three parameters, the discharge coefficient C_D, the non-axial kinetic energy E_k and the turbulent kinetic energy T_{ke}. These three parameters are defined in Table 2.

RESULTS

Fig. 2. Comparison between calculated and measured discharge coefficient (injector series S1)

Figure 2 presents the measured discharge coefficients obtained for the S1 injector series as a function of the injection pressure. It can be observed in this figure that the discharge coefficient is influenced neither by the injection pressure nor by the eccentricity of the nozzle for the injector series S1. Similar results were obtained for the two other nozzle series (S2 and S3) and for all nozzle configurations and injection pressure the measured discharge coefficient is found constant of the order of 0.7.

Figure 2 also presents the calculated discharge coefficients for the injector series S1. As for the measurements, the calculations report that the discharge coefficient is not a function of the injection pressure. As far as the influence of the nozzle geometry is concerned, the calculation results indicate a slightly greater discharge coefficient for the injector S1I1 while it is constant for the three other nozzles. However, the agreement between the calculations and the measur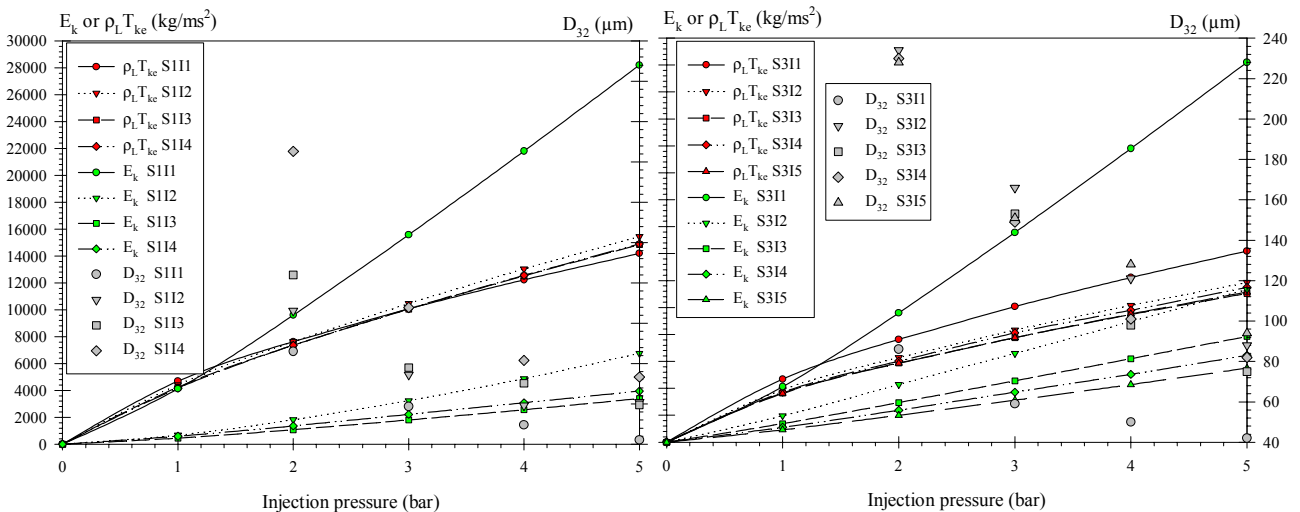ements is acceptable and allows us concluding that the calculations are well adapted to represent the flow that develops inside the nozzle. A similar agreement was found for the two other injector series.

The flow that develops in the simplified cavity nozzle is rather complex. It was presented in a previous paper [8]. The internal flow is divided in two flows. A part of the flow goes as directly as possible from disk 1 to disk 3 and the rest of the flow follows helical paths in disk 2 before reaching disk 3. The proportion of the direct flow may be considerably reduced when the nozzle eccentricity is high. The combination of these two flow components at the nozzle orifice leads to the development of a double-swirl flow. Similar flows were reported for compound nozzles by previous studies [5, 7]. The issuing double-swirl flow is characterised by the parameter E_k defined in table 2. This parameter was found interesting in the work reported by Ren and Sayar [7]. Beside this parameter, the issuing liquid flow is characterised by the turbulent kinetic energy T_{ke} defined in the previous section. As explained in the introduction, many studies of the literature reported that the atomisation propensity of compound nozzles is directly related to the turbulent level at the nozzle exit. This very point is discussed through the results presented in Figures 3 and 4.

Figure 3 presents the issuing flow characteristics E_k and T_{ke} as a function of the injection pressure for the nozzle series S1. This figure shows that both characteristics are very much influenced by the injection pressure. The turbulent kinetic energy increases almost linearly with the injection pressure as reported by Glodowski et al. [4] and the non-axial kinetic energy also increases with the injection pressure. As far as the influence of the nozzle geometry is concerned, the two issuing flow characteristics report very different behaviours. Indeed, whereas T_{ke} is almost constant for the four nozzles of the series S1, E_k is very much a function of the nozzle eccentricity. The nozzle configurations examined here report a decrease of E_k as the eccentricity increases. It must be added that this dependence is a function of the cavity disk thickness. Indeed, despite a similar behaviour is obtained for the injector series S2, the increase of E_k with the

Fig. 3 (left). Issuing flow characteristics E_k and T_{ke} and measured Sauter mean diameter D_{32} (Injector series S1)
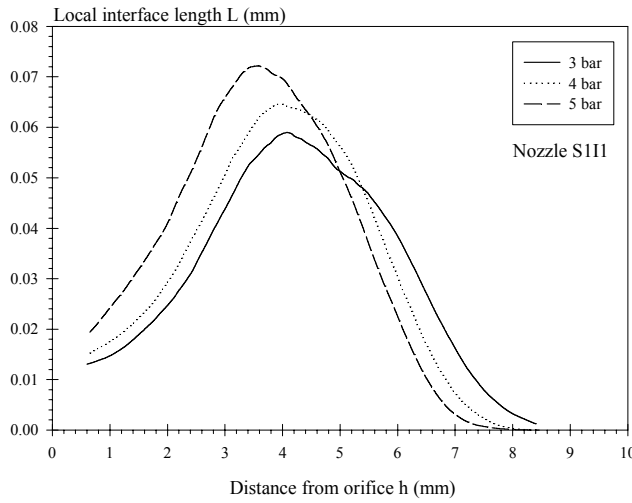**Fig. 4 (right).** Issuing flow characteristics E_k and T_{ke} and measured Sauter mean diameter D_{32} (Injector series S3)

nozzle eccentricity is far less pronounced and, for all injection pressures and nozzle eccentricities, E_k is less than $\rho_L T_{ke}$ for the S2 nozzles. For the S1 series, Fig. 3 indicates a much higher value of E_k for the S1I1 configuration.
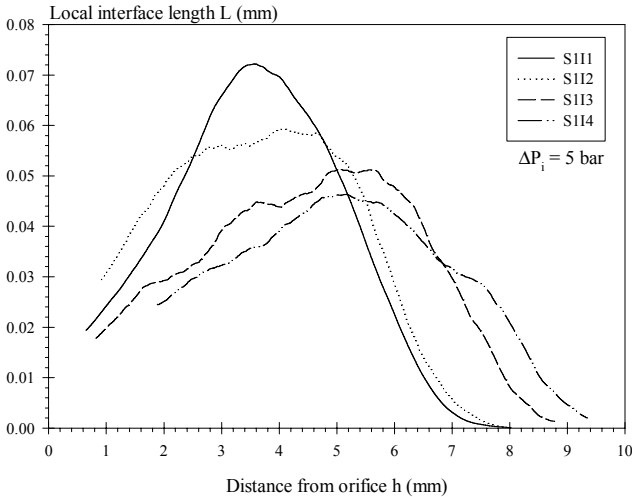
Figure 3 shows also the measured Sauter mean diameter D_{32} measured for all S1 nozzles as a function of the injection pressure. It must be first noted that this diameter depends on the injection pressure and on the nozzle geometry. This result is very important and agrees with Glodowski et al conclusion [4] that says that the turbulence is not solely responsible of the atomisation of liquid flow issuing from cavity nozzle. Indeed, while the turbulent level is kept constant as the nozzle eccentricity increases, the Sauter mean diameter considerably decreases. Furthermore, bearing in mind that the issuing mean liquid flow is independent of the nozzle geometry (see Fig. 2), it appears that the atomisation process is also influenced by the non-axial flow at the nozzle exit characterised here by the parameter E_k.

Figure 4 presents the same results for the injector series S3. This figure shows that an increase of the disk 2 thickness induces a decrease of both E_k and T_{ke}. However, it can be noted that E_k varies much more than T_{ke} that is almost constant for high disk 2 thicknesses. This behaviour is accompanied by an increase of the mean diameter D_{32}. Thus, the results presented in Figures 3 and 4 indicate that the atomisation process of low-Weber liquid flows is a function of the turbulence and of the non-axial flow at the nozzle exit. Globally speaking, the atomisation is enhanced thanks to an increase of these two parameters.

As explained in the introduction, one of the objectives of this work is to characterise the perturbed liquid flow during the atomisation process by measuring the local interface length L. The method used to measure L is explained in the previous section. It has to be kept in mind that this length is representative of the local interface perturbations. Figure 5 presents an example of the spatial evolution of the local interface length obtained for the nozzle S1I1 for three injection-pressures. The smooth evolution of the length L is due to the fact that at each position, the length presented is the average of the 100 values obtained before and after this position.

Fig. 5. Evolution of the local interface length with the distance from the orifice. Influence of the injection pressure (Nozzle S1I1)

Fig. 6. Evolution of the local interface length with the distance from the orifice. Influence of the eccentricity of the nozzle ($\Delta P_i = 5$ bar)

Figure 5 shows that the local interface length increases up to a maximum (L_m) and then decreases to reach zero at a distance from the nozzle. The increase of L is due to the presence of perturbations whose growth induces an increase of the liquid gas interface. The decrease of L corresponds to the location at which the break-up of the bulk flow occurs. This indicates that the break-up reduces the local tortuosity of the local interface. Thus, as expected, the liquid atomisation reduces the liquid gas interface area. The spatial evolution of L indicates the beginning of the disintegration process ($L = L_m$) and the position at which it is completed ($L = 0$).

The spatial evolution of the local interface length is a function of the injection pressure. Figure 5 shows that as the injection pressure increases, the perturbations grow faster, the disintegration starts sooner and is completed at a shorter distance from the orifice. Bearing in mind that the aerodynamic forces have no effect in the present case, the influence of the injection pressure is due to a variation of the issuing flow characteristics, namely, E_k and T_{ke} (see Fig. 3).

Figure 6 presents the spatial evolution of the local interface length at 5 bar for the injector series S1 (influence of the eccentricity). It can be seen that the injector geometry influences the evolution of the local interface length. When the eccentricity increases, the characteristic value L_m decreases. Furthermore, the atomisation process is delayed and is completed farther from the nozzle. Bearing in mind that the turbulent level in the issuing flow is almost independent of the nozzle geometry (see Fig. 2), the variation of the spatial evolution of L shown in Fig. 6 is mainly due to a variation of the non axial kinetic energy of the issuing liquid flow. This confirms the paramount influence of the non-axial issuing flow component on the atomisation process.
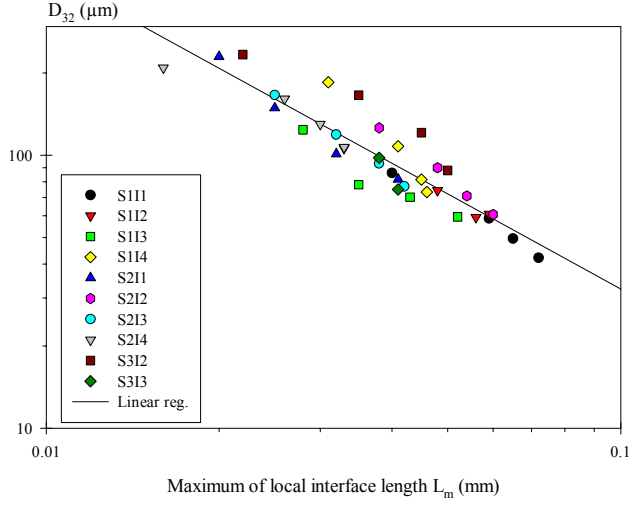
The comparison of the results presented in Figures 3, 5 and 6 shows that the mean diameter decreases when L_m increases. This behaviour indicates that the characteristic L_m is well representative of the atomisation process. This result is confirmed by Fig. 7 that presents the mean diameter D_{32} versus the maximum local length L_m for all nozzle configurations and all tested injection pressures. It appears in this figure that the relationship between L_m and D_{32} is a function neither of the injection pressure nor of the nozzle geometry. This result is very important for the two following reasons.

Fig. 7: Relation between the maximum interface local length L_m and the Sauter mean diameter D_{32} (all nozzles, all injection pressures)
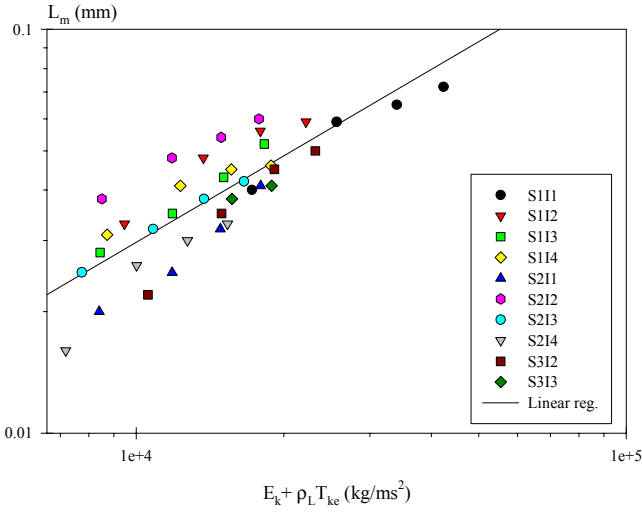
Fig. 8. Relationship between the maximum of local interface length L_m and the issuing flow characteristics $(E_k + \rho_L T_{ke})$ (all nozzles, all injection pressures)
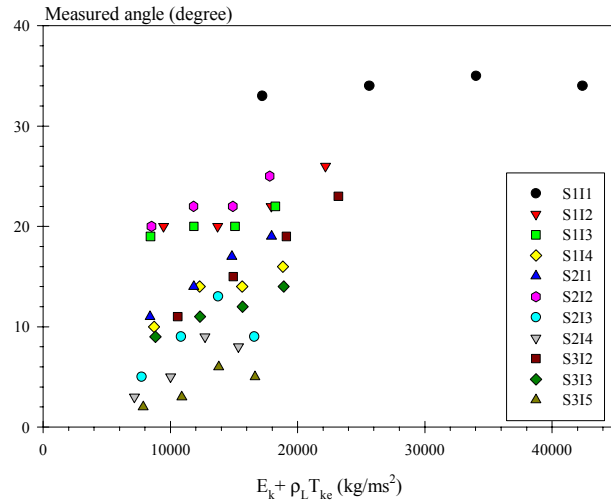
Fig. 9. Relationship between the measured angle and the issuing flow characteristics $(E_k + \rho_L T_{ke})$ (all nozzles, all injection pressures)

First, it confirms the relevance of the characteristic L_m as far as the atomisation process is concerned. Second, it invites us to study the influence of the issuing flow characteristics E_k and T_{ke} on the maximum local interface length L_m rather than on the mean diameter D_{32}.

The different results issued from this study indicate that the energy brought to the fluid is divided in two parts. One part is transmitted to the fluid as flowing energy. This energy is characterised by the discharged coefficient. The constant discharge coefficients obtained here for all nozzles and for all injection pressures indicate that the flowing energy is a constant proportion of the incident energy. As the mean liquid velocity is small, the flowing energy does not participate to the atomisation process. The part of the incident energy that is used in the atomisation process is a function of the non-axial kinetic energy and of the turbulent kinetic energy of the issuing flow. Therefore, the energy dedicated to atomisation is likely to be a proportion of the pressure energy described by the parameter $(E_k + \rho_L T_{ke})$.

Figure 8 shows the evolution of the maximum local interface length L_m as a function of $(E_k + \rho_L T_{ke})$. The single behaviour reported by this figure that contains the results obtained for all nozzles and for all injection pressures validates the fact that the atomisation process depends on the issuing flow parameter $(E_k + \rho_L T_{ke})$ only. When this parameter increases, the maximum of local interface length increases leading to a decrease of the Sauter mean diameter according to Fig. 7. This result is of paramount importance. It shows that, at low Weber number, the geometry of the nozzle can be optimised by maximizing both the non-axial kinetic energy and the turbulent kinetic energy of the issuing liquid flow.

Previous studies [7, 8] suggested that the influence of the non-axial flow component on the drop size was mainly due to a modification of the shape of the jet issuing from the nozzle. Indeed, the presence of the non-axial flow component at the nozzle exit induces an expansion of the jet in the plane of symmetry of the nozzle (plane of Fig. 1). The issuing liquid flow evolves from a cylindrical liquid jet to a flat liquid sheet as the non-axial kinetic energy increases. For a given amount of liquid, the characteristic length of a sheet (the thickness) is much smaller than the one of a cylindrical jet (the diameter). Thus, the influence of the non-axial kinetic energy on the shape of the issuing liquid flow favours the production of smaller drops. If the role of the non-axial liquid flow on the spray characteristics is limited to an influence on the issuing jet shape, the angle of the liquid flow just at the nozzle exit would mainly depend on the same parameter as the atomisation process, namely, the parameter $(E_k + \rho_L T_{ke})$. The angle of the issuing liquid flow was measured as close as possible to the nozzle exit. The measurements used an image analysing technique that was applied on a high number of images for all working conditions. Figure 9 shows the evolution of the measured angle with the parameter $(E_k + \rho_L T_{ke})$ for all nozzles and all injection pressures.

It can be seen that the angle of the issuing liquid jet is not only a function of the parameter $(E_k + \rho_L T_{ke})$ and that the nozzle geometry affects the value of the angle as well. This demonstrates that, although the parameter $(E_k + \rho_L T_{ke})$ influences the aperture angle of the jet, it also influences the perturbation growth on the liquid gas interface as well as the subsequent atomisation process and drop size distribution of the resulting spray.

CONCLUSION

Numerous conclusions can be drawn from this study that investigates the problem of liquid atomisation in gas environment at low Weber number. In this specific situation, the aerodynamic forces due to the interaction between the liquid and the gas have no effect on the atomisation process that is mainly controlled by the issuing liquid flow. By conducting a numerical investigation of the internal liquid flow on simplified cavity nozzles as well as an experimental study on their behaviour, it is found that the atomisation process is influenced by two issuing flow characteristics, namely, the non-axial flow kinetic energy and the turbulent kinetic energy. Thus, the improvement of the geometry of nozzles based on the concept of a turbulent cavity can be achieved by maximising both the turbulent energy level and the energy contained in the non-axial liquid flow component. This result applies for compound injectors for instance. Indeed, although the nozzles investigated within the scope of this study are very simplified compared to compound nozzles, the relationships between the injection pressure, the turbulent level and the Sauter mean diameter obtained here are similar to those reported in the literature. Thus, the behaviour of the nozzles tested in the present work is very much alike the one of compound nozzles.

All the works reported in the literature on the influence of the nozzle geometry on the atomisation efficiency relate calculated issuing flow characteristics to a measured mean drop size neglecting the important step of liquid flow perturbation. In the present study, an experimental characterisation of the liquid flow during the atomisation phase is performed. It is based on the measurement of the liquid gas interface length as a function of the distance from the nozzle. The results show the relevance of the approach. Indeed, the spatial evolution of the interface length makes appear a maximum L_m that is likely representative of the beginning of the atomisation process and that is solely related to the Sauter mean diameter and to the maximum energy available for atomisation, namely, $(E_k + \rho_L T_{ke})$. This finding is important. First, it allows showing that the influence of the non-axial liquid flow component on the atomisation process is not limited to a modification of the issuing liquid flow geometry. Second, from a more general point of view, it suggests that the approach that consists in describing liquid atomisation processes as a problem of liquid surface balance is relevant and very promising.

NOMENCLATURE

C_D	Discharge coefficient (-)
D_{32}	Sauter mean diameter (µm)
E_k	Kinetic energy of the non axial flow at the nozzle exit (kg/ms^2)
h	Distance from nozzle orifice (mm)
L	Local interface length (mm)
L_m	Maximum of local interface length (mm)
Q_v	Volume flow rate (m^3/s)
S	Exit orifice section (m^2)
T_{ke}	Mean turbulent kinetic energy at the nozzle exit (m^2/s^2)
(u, v, w)	Velocity component (m/s)
(u', v', w')	Turbulent velocity fluctuations (m/s)
vol_j	Volume of the jth cell in the exit section (m^3)
ΔP_i	Injection pressure (bar)
ρ_L	Liquid density (kg/m^3)

REFERENCE

1. F.Q. Zhao and M.C. Lai, The Spray Characteristics of Automotive Port Fuel Injection – A Critical Review, SAE Technical Paper Series 950506, 1995
2. S. Parrish and L. Evers, Spray Characteristics of Compound Silicon Micro Machined Port Fuel Injector Orifices, SAE Technical Paper Series 950510, 1995
3. S.M. Rivette and L.W. Evers, Compound Port Fuel Injector Nozzle Droplet Sizes and Spray Patterns, SAE Technical Paper Series 960114, 1996
4. M.L Glodowski, D.J. Michalek and L.W. Evers, The Use of Results from Computational Fluid Dynamic Fuel Injector Modeling to Predict Spray Characteristics, SAE Technical Paper Series 961191, 1996
5. J. Heyse, F. Schatz, B. Ader, J. Schlerfer and S. Haubold, Electroformed Multilayer Orifice Plate for Improved Fuel Injection Characteristics, SAE Technical Paper Series 971070, 1997
6. D.J. Michalek, B.D. Peschke and L.W. Evers, Computational Design of Experiments for Compound Fuel Injector Nozzles, SAE Technical Paper Series 971617, 1997
7. W.M. Ren and H. Sayar, Influence of Nozzle Geometry on Spray Targeting and Atomization for Port Fuel Injector, SAE Technical Paper Series 2001-0608, 2001
8. K. Triballier, J. Cousin and C. Dumouchel, Relations Between Internal Flow Structures and Disintegration Processes in Spray Formation, Proc. ILASS-Europe 2002, Zaragoza, 2002